The difference in slope between the XMCD curves indicates that the Gd and Fe moments gradually tilt from the field direction at different rates. A quantitative evaluation suggested that the Fe moments tilt about three times as fast as the Gd moments as the magnetic field increases. Hence, the compensation between such Gd and Fe moments results in an increase in the bulk magnetization. This behavior is consistent with theoretical prediction, what we call the bulk-twisted state, that the effective exchange coupling between the spins in different layers and the Zeeman energy of the spins in an external field compete with each other [2].

The most important finding is a characteristic sharp peak appearing at a coercive field $H_c = \pm 50$ Oe soon after the magnetic field is reversed. No indication associated with the peak is observed in the magnetization curve. A possible spin state corresponding to this peak is an Fe-aligned state, where Fe moments are dominant and parallel and where Gd moments are antiparallel to the field direction. Since the Zeeman energies of the Gd and the Fe moments are completely canceled out at H_c, the antiferromagnetic exchange coupling at the interfaces between the Gd and Fe layers plays an important role in determining the magnetic structure, although the effect of the magnetic anisotropy cannot be disregarded.

In conclusion, magnetic hysteresis measurements of XMCD have precisely revealed the magnetization process of each element in Gd/Fe multilayers, which is impossible by magnetization measurements. These results show the indispensable availability of XMCD measurements with the polarization modulation technique, for the study of magnetism in complicated materials.

Akihisa Koizumi, Masafumi Takagaki and Nobuhiko Sakai
Himeji Institute of Technology

E-mail: akihisa@sci.himeji-tech.ac.jp

References

[1] M. Suzuki et al., to be published in *Jpn. J. Appl. Phys.*

[2] J. G. LePage and R. E. Camly, *Phys. Rev. Lett.* **65** (1990) 1152.

XMCD SPECTRUM AT PT $L_{2,3}$ EDGES RECORDED BY HELICITY MODULATION TECHNIQUE

X-ray magnetic circular dichroism (XMCD) at the Pt $L_{2,3}$ edge is a powerful tool for studying the magnetic properties of Pt 5*d* bands and sensitively reflects the TM 3d states in ferromagnetic TM-Pt_3 intermetallics (TM: transition-metal). We previously found that the Pt 5*d* magnetic states in MnPt3 have a quenched orbital component and are dominated by the spin character, whereas a main contribution in $CrPt_3$ is carried by the orbital moment rather than the spin component and the Pt moments couple antiferromagnetically with Cr moments [1].

To study this contrasting magnetic property, the Pt *L* edge XMCD in $(Cr_{1-X}Mn_X)Pt_3$ mixed crystal system is informative for a better understanding of the 3*d* magnetic states. In particular, we are interested in the crossover from orbital to spin character at an intermediate region, where the Pt magnetic moments will be quenched. The helicity-modulation technique [2] recently developed has been applied for measuring weak XMCD signals with a high accuracy. A synthetic diamond (111) crystal slab 0.73 mm thick is operated around the 220 reflection in the Laue geometry. The photon helicity is switched fast between plus and minus offset angles around the Bragg condition, which was previously determined from polarization measurements of the transmitted beam, as shown in Figure 1. In the energy range of the Pt $L_{2,3}$ edges, the photon helicity is alternately turned at 200 Hz by flipping between the offset angles of ±20 arcseconds.

Figures 2 and 3 show Pt L_3 and L_2 edge XMCD spectra, aligned at the absorption edge energy, in a $(Cr_{1-X}Mn_X)Pt_3$ mixed crystal system. When the Mn content is increased, the L_3 edge XMCD is systematically changed from positive to negative, and a dispersion type profile is observed in the intermediate range. This trend is interpreted as an increase in the volume fraction of ferromagnetic $MnPt_3$ in ferrimagnetic $CrPt_3$.

On the other hand, the L_2 edge XMCD always keeps a positive sign and shows a small amplitude at $(Cr_{0.5}Mn_{0.5})Pt_3$, which indicates the collapse of the Pt 5*d* magnetic moments. The L_3 (L_2) spectrum with a negative (positive) sign means that the Pt 5*d* moments ferromagnetically couple with the 3*d* moments of the TM partner, whereas the positive L_3 edge XMCD on the Cr-rich side shows that the Pt moments dominantly arise from the orbital character, and that such a situation is maintained even by the substitution of Mn for Cr atoms. These spectra can be basically reproduced by the Lorentzian line-shape.

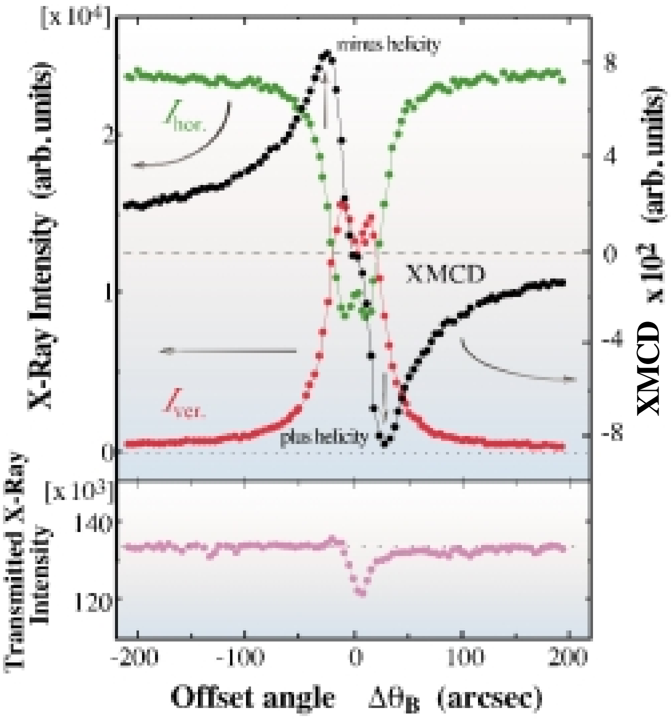

Fig.1: Measured variations of X-ray intensities versus the offset with respect to the Bragg angle in the energy range of 11 keV. The polarization state of the transmitted X-ray is converted into circular polarization at ±20 arcseconds. The XMCD amplitude was also monitored as a function of the offset angle at the Pt L_3 edge in 61.5at% Pt-Fe alloy. The XMCD sign is negative at the L_3 edge in ferromagnet, so that the minus helicity is obtained at the minus offset angle.

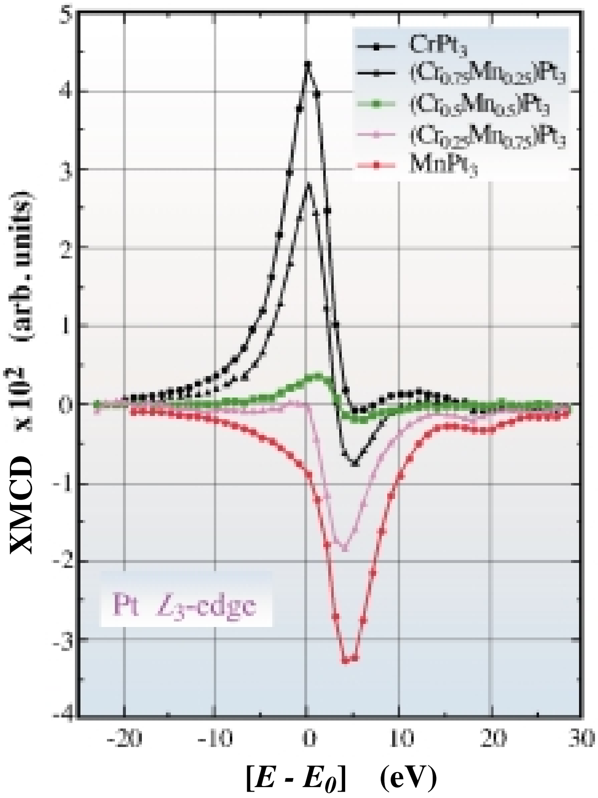

Fig.2: XMCD spectrum at the Pt L_3 edge.

To estimate the Pt magnetic properties using the sum rules [3], the standard procedure is applied for evaluating the intensity of the XMCD and XANES white-line [1], and the ground-state expectation values of orbital and spin moments are empirically obtained.

Figure 4 shows the dependence of Pt magnetic moments on the Mn content. We can see that the orbital moment in $MnPt_3$ is almost quenched,

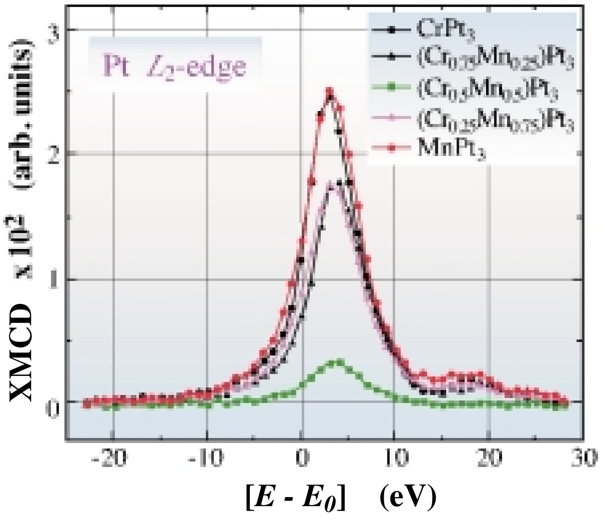

Fig.3: XMCD spectrum at the Pt L_2 edge.

whereas a relatively large orbital component remains in CrPt$_3$. The spin component always shows a positive moment in spite of the small amplitude on the Cr-rich side, as a result, the total moment increases linearly with the Mn content. In (Cr$_{0.5}$Mn$_{0.5}$)Pt$_3$, the total moment is, however, almost cancelled out due to the opposite contribution between the orbital and spin characters, so that this sample has a relatively low Curie temperature.

The Pt *L* edge XMCD provides the evidence that the Pt 5*d* magnetic states sensitively depend on the neighboring TM atom and local environment. The magnetic properties of the (Cr$_{1-x}$Mn$_x$)Pt$_3$ system can be explained by taking the average over the volume fractions of ferromagnetic MnPt$_3$ and ferrimagnetic

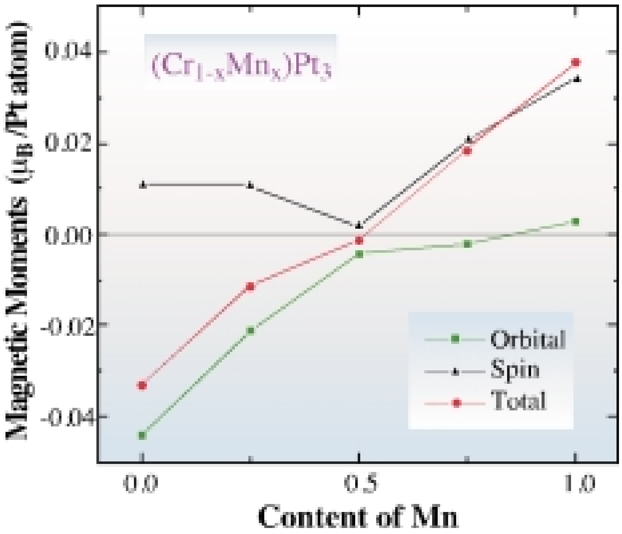

Fig.4: Orbital, spin and total magnetic moments of Pt atom estimated from the sum rules. These data are subjected to no correction for the saturation magnetization.

Hiroshi Maruyama
Okayama University

E-mail: maruyama@mag.okayama-u.ac.jp

References

[1] H. Maruyama *et al., J. Magn. Magn. Mater.* **43** (1995) 140.

[2] M. Suzuki *et al., Jpn. J. Appl. Phys.* **37** (1998) L1488.

[3] P. Carra *et al., Phys. Rev. Lett.* **70** (1993) 694.

HIGH RESOLUTION Ce 3*d*-4*f* RESONANT PHOTOEMISSION STUDY OF CeNiSn and CePdSn

Many Ce compounds have attracted interest widely due to their strongly correlated Ce 4*f* states hybridized with valence band states. High resolution photoemission spectroscopy is a useful technique to experimentally reveal the electronic states. It is known, however, that rare-earth 4*f* electronic states on the surface are remarkably different from those in bulk. Measurements at low $h\nu$ (< 200 eV) cannot faithfully probe the bulk Ce 4*f* states due to their surface-sensitivity.

In order to study such bulk electronic states using high energy excitations ($h\nu$ > 500 eV), a high resolution photoemission station has been constructed at the twin-helical undulator beamline **BL25SU** [1]. Here, we report high resolution Ce 3*d* resonant photoemission spectra of CeNiSn and CePdSn measured at this station.

CeNiSn is a so-called "Kondo semiconductor" where the Kondo temperature (T_K) is of the order of ~40 K and the Ce 4*f* electrons are valence-fluctuating [2]. For CePdSn, on the other hand, the Ce 4*f* electrons are more localized and T_K is thought to be lower than 7 K [3]. A Ce 3*d* resonant photoemission study was performed with the total energy resolution of ~0.22 eV, as shown in Figure 1**(b)**. The sample temperature was about 20 K.

Figure 1**(a)** shows Ce 3*d* resonant valence band spectra of CeNiSn and CePdSn together with the Ce 4d resonance spectra. The Ce 4*f* contributions are obtained by subtracting the Ce 3*d* off resonance ($h\nu \leq$ 875 eV) spectra from the on resonance ($h\nu$ ~882 eV) ones ("3*d*-4*f* spectra"). In the 3*d*-4*f* spectra of CeNiSn, one can see a strong peak due to the f^1 final states near E_F and the shoulder structure of the f^0 final states at ~2.4 eV. For CePdSn, the f^0 peak at about 1.9 eV and the f^1 peak near E_F, which is comparable to slightly stronger than the f^0 peak, are observed.

The Ce 4*f* contributions obtained by the same procedure in the Ce 4*d* resonance region ($h\nu$ ~120 eV, "4*d*-4*f* spectra") are also displayed. They were measured at beamline BL-3B of the Photon Factory. One can notice that the 4*d*-4*f* spectral shapes are